Smooth Adaptation by Sigmoid Shrinkage

Abdourrahmane Atto, Dominique Pastor, Grégoire Mercier

Smooth Adaptation by Sigmoid Shrinkage

Abdourrahmane M. Atto * Dominique Pastor †
Grégoire Mercier ‡
Institut TELECOM - TELECOM Bretagne
Lab-STICC - CNRS, UMR 3192
Technopôle Brest-Iroise
CS 83818 - 29238
Brest Cedex 3 - France

Abstract

This work addresses the properties of a sub-class of sigmoid based shrinkage functions: the non zero-forcing smooth sigmoid based shrinkage functions or SigShrink functions. It provides a SURE optimization for the parameters of the SigShrink functions. The optimization is performed on an unbiased estimation risk obtained by using the functions of this sub-class. The SURE SigShrink performance measurements are compared to those of the SURELET (SURE linear expansion of thresholds) parameterization. It is shown that the SURE SigShrink performs well in comparison to the SURELET parameterization. The relevance of SigShrink is the physical meaning and the flexibility of its parameters. The SigShrink functions perform weak attenuation of data with large amplitudes and stronger attenuation of data with small amplitudes, the shrinkage process introducing little variability among data with close amplitudes. In the wavelet domain, SigShrink is particularly suitable for reducing noise without impacting significantly the signal to recover. A remarkable property for this class of sigmoid based functions is the invertibility of its elements. This property makes it possible to smoothly tune contrast (enhancement - reduction).

Keywords: Shrinkage; Sigmoid; Wavelet.

1 Introduction

The Smooth Sigmoid-Based Shrinkage (SSBS) functions introduced in [8] constitute a wide class of WaveShrink functions. The WaveShrink (Wavelet Shrinkage) estimation of a signal involves projecting the observed noisy signal on a wavelet basis, estimating the signal coefficients with a thresholding or shrinkage function and reconstructing an estimate of the signal by means of the inverse wavelet transform of the shrunken wavelet coefficients. The SSBS functions derive from the sigmoid function and perform an adjustable wavelet shrinkage thanks to parameters that control the attenuation degree imposed to the wavelet coefficients. As a consequence, these functions allow for a very flexible shrinkage.

* *am.atto@telecom-bretagne.eu*
† *dominique.pastor@telecom-bretagne.eu*
‡ *gregoire.mercier@telecom-bretagne.eu*

The present work addresses the properties of a sub-class of the SSBS functions, the non-zero-forcing SSBS functions, hereafter called the SigShrink (Sigmoid Shrinkage) functions. First, we provide a discussion on the optimization of the SigShrink parameters in the context of WaveShrink estimation. The optimization exploits the new SURE (Stein Unbiased Risk of Estimation, [22]) proposed in [16]. SigShrink performance measurements are compared to those obtained when using the parameterization of [16], which consists of a sum of Derivatives Of Gaussian (DOGs). We then address the main features of the SigShrink functions: artifact-free denoising and smooth contrast functions make SigShrink a worthy tool for various signal and image processing applications.

The presentation of this work is as follows. Section 2 presents the SigShrink functions. Section 3 briefly describes the non-parametric estimation by wavelet shrinkage and addresses the optimization of the SigShrink parameters with respect to the new SURE approach described in [16]. Section 4 discusses the main properties of the SigShrink functions by providing experimental tests. These tests assess the quality of the SigShrink functions for image processing: adjustable and artifact-free denoising, as well as contrast functions. Finally, section 5 concludes this work.

2 Smooth sigmoid-based shrinkage

The family of real-valued functions defined by [8]:

$$\delta_{\tau,\lambda}(x) = \frac{x}{1+e^{-\tau(|x|-\lambda)}}. \tag{1}$$

for $x \in \mathbb{R}$, $(\tau,\lambda) \in \mathbb{R}_+^* \times \mathbb{R}_+$, are shrinkage functions satisfying the following properties.

(P1) **Smoothness**: of the shrinkage function so as to induce small variability among data with close values;

(P2) **Penalized shrinkage**: a strong (resp. a weak) attenuation is imposed for small (resp. large) data.

(P3) **Vanishing attenuation at infinity**: the attenuation decreases to zero when the amplitude of the coefficient tends to infinity.

Each $\delta_{\tau,\lambda}$ is the product of the identity function with a sigmoid-like function. A function $\delta_{\tau,\lambda}$ will hereafter be called a SigShrink (Sigmoid Shrinkage) function.

Note that $\delta_{\tau,\lambda}(x)$ tends to $\delta_{\infty,\lambda}(x)$, which is a hard-thresholding function defined by:

$$\delta_{\infty,\lambda}(x) = \begin{cases} x\mathbb{1}_{\{|x|>\lambda\}} & \text{if} \quad x \in \mathbb{R}\setminus\{-\lambda,\lambda\}, \\ \pm\lambda/2 & \text{if} \quad x = \pm\lambda, \end{cases} \tag{2}$$

where $\mathbb{1}_\Delta$ is the indicator function of a given set $\Delta \subset \mathbb{R}$: $\mathbb{1}_\Delta(x) = 1$ if $x \in \Delta$; $\mathbb{1}_\Delta(x) = 0$ if $x \in \mathbb{R}\setminus\Delta$. It follows that λ acts as a threshold. Note that $\delta_{\infty,\lambda}$ sets a coefficient with amplitude λ to half of its value and so, minimizes the local variation (second derivative) around λ, since $\lim_{x\to\lambda^+}\delta_{\infty,\lambda}(x) - 2\delta_{\infty,\lambda}(\lambda) + \lim_{x\to\lambda^-}\delta_{\infty,\lambda}(x) = 0$.

In addition, it is easy to check that, in Cartesian-coordinates, the points $A = (\lambda,\lambda/2)$, $O = (0,0)$ and $A' = (-\lambda,-\lambda/2)$ belong to the curve of the function $\delta_{\tau,\lambda}$ for every $\tau > 0$. Indeed, according to Eq. (1), we have $\delta_{\tau,\lambda}(\pm\lambda) = \pm\lambda/2$ and $\delta_{\tau,\lambda}(0) = 0$ for any $\tau > 0$. It follows that τ parameterizes the curvature of the arc $\widehat{A'OA}$, that is, the arc of the SigShrink function in the interval $]-\lambda,\lambda[$. This curvature directly relates to

the attenuation degree we want to apply to the wavelet coefficients. Consider the graph of figure 1, where a SigShrink function is plotted in the positive half plan. Due to the antisymmetry of the SigShrink function, we only focus on the curvature of arc $\widehat{OA}$. Let C be the intersection between the abscissa axis and the tangent at

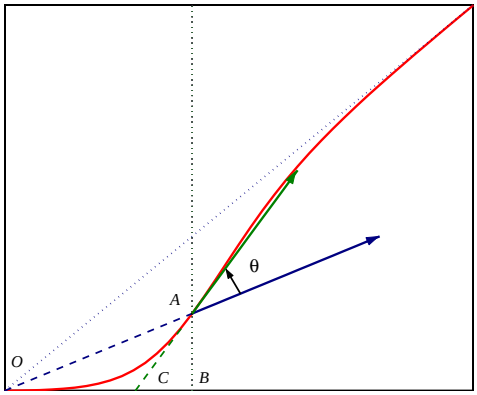

Figure 1: Graph of $\delta_{\tau,\lambda}$ in the positive half plan. The points A, B and C represented on this graph are such that $A = (\lambda, \lambda/2)$, $B = (\lambda, 0)$ and C is the intersection between the abscissa axis and the tangent to $\delta_{\tau,\lambda}$ at point A.

point A to the curve of the SigShrink function. The equation of this tangent is $y = 0.25(2+\tau\lambda)(x-\lambda)+0.5\lambda$. The coordinates of point C are $C = (\tau\lambda^2/(2+\tau\lambda), 0)$. We can easily control the arc $\widehat{OA}$ curvature via the angle, denoted by θ, between vector $\overrightarrow{OA}$, which is fixed, and vector $\overrightarrow{CA}$, which is carried by the tangent to the curve of $\delta_{\tau,\lambda}$ at point A. The larger θ, the stronger the attenuation of the coefficients with amplitudes less than or equal to λ. For a fixed λ, the relation between angle θ and parameter τ is

$$\cos\theta = \frac{\overrightarrow{OA}.\overrightarrow{CA}}{||\overrightarrow{OA}||.||\overrightarrow{CA}||} = \frac{10+\tau\lambda}{\sqrt{5(20+4\tau\lambda+\tau^2\lambda^2)}}. \tag{3}$$

It easily follows from Eq. (3) that $0 < \theta < \arccos(\sqrt{5}/5)$; when $\theta = \arccos(\sqrt{5}/5)$, then $\tau = +\infty$ and $\delta_{\tau,\lambda}$ is the hard-thresholding function of Eq. (2). From Eq. (3), we derive that $\tau = \tau(\theta,\lambda)$ can be written as a function of θ and λ as follows:

$$\tau(\theta,\lambda) = \frac{10}{\lambda}\,\frac{\sin^2\theta + 2\sin\theta\cos\theta}{5\cos^2\theta - 1}. \tag{4}$$

In practice, when λ is fixed, the foregoing makes it possible to control the attenuation degree we want to impose to the data in $]0,\lambda[$ by choosing θ, which is rather natural, and calculating τ according to Eq. (4). Since we can control the shrinkage by choosing θ, $\delta_{\theta,\lambda} = \delta_{\tau(\theta,\lambda),\lambda}$ henceforth denotes the SigShrink function where $\tau(\theta,\lambda)$ is given by Eq. (4). This interpretation of the SigShrink parameters makes it easier to find "nice" parameters for practical applications. Summarizing, the SigShrink computation is performed in three steps:

1. Fix threshold λ and angle θ of the SigShrink function, with $\lambda > 0$ and $0 < \theta < \arccos(\sqrt{5}/5)$. Keep in mind that the larger θ, the stronger the attenuation.

2. Compute the corresponding value of τ from Eq. (4).

3. Shrink the data according to the SigShrink function $\delta_{\tau,\lambda}$ defined by Eq. (1).

Hereafter, the terms "attenuation degree" and "threshold" designate θ and λ, respectively. In addition, the notation $\delta_{\tau,\lambda}$ will be preferred for calculations and statements. The notation $\delta_{\theta,\lambda}$, introduced just above, will be used for practical and experimental purposes since the attenuation degree θ is far more natural in practice that parameter τ. Some SigShrink graphs are plotted in figure 2 for different values of the attenuation degree θ (fixed threshold λ).

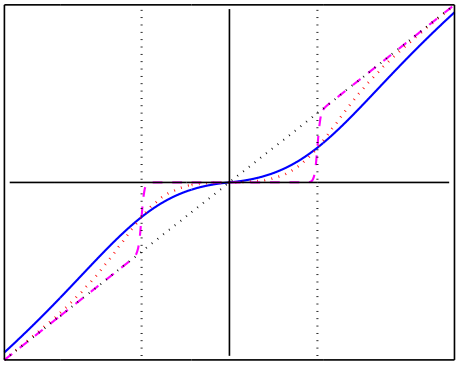

Figure 2: Shapes of SigShrink functions for different values of the attenuation degree θ: $\theta = \pi/6$ for the continuous (blue) curve, $\theta = \pi/4$ for the dotted (red) curve, and $\theta = \pi/3$ for the dashed (magenta) curve.

3 Sigmoid shrinkage in the wavelet domain

3.1 Estimation via shrinkage in the wavelet domain

Let us recall the main principles of the non-parametric estimation by wavelet shrinkage (the so-called WaveShrink estimation) in the sense of [13]. Let $\boldsymbol{y} = \{y_i\}_{1\leqslant i\leqslant N}$ stand for the sequence of noisy data $y_i = f(t_i) + e_i$, $i = 1,2,\ldots,N$, where f is an unknown deterministic function, the random variables $\{e_i\}_{1\leqslant i\leqslant N}$ are independent and identically distributed (iid), Gaussian with null mean and variance σ^2, in short, $e_i \sim \mathcal{N}(0,\sigma^2)$ for every $i = 1,2,\ldots,N$.

In order to estimate $\{f(t_i)\}_{1\leqslant i\leqslant N}$, we assume that an orthonormal transform, represented by an orthonormal matrix $\mathcal{W}$, is applied to $\boldsymbol{y}$. The outcome of this transform is the sequence of coefficients

$$c_i = d_i + \epsilon_i, \qquad i = 1,2,\ldots,N, \tag{5}$$

where $\boldsymbol{c} = \{c_i\}_{1\leqslant i\leqslant N} = \mathcal{W}\boldsymbol{y}$, $\boldsymbol{d} = \{d_i\}_{1\leqslant i\leqslant N} = \mathcal{W}\boldsymbol{f}$, $\boldsymbol{f} = \{f(t_i)\}_{1\leqslant i\leqslant N}$ and $\boldsymbol{\epsilon} = \{\epsilon_i\}_{1\leqslant i\leqslant N} = \mathcal{W}\boldsymbol{e}$, $\boldsymbol{e} = \{e_i\}_{1\leqslant i\leqslant N}$. The random variables $\{\epsilon_i\}_{1\leqslant i\leqslant N}$ are iid and $\epsilon_i \sim \mathcal{N}(0,\sigma^2)$. The transform $\mathcal{W}$ is assumed to achieve a sparse representation of the signal in the sense that, among the coefficients d_i, $i = 1,2,\ldots,N$, only a few of them have large amplitudes and, as such, characterize the signal. In this respect, simple estimators such as "keep or kill" and "shrink or kill" rules are proved to be nearly optimal, in the Mean Square Error (MSE) sense, in comparison with oracles (see [13] for further details). The wavelet transform is sparse in the sense given

above for smooth and piecewise regular signals [13]. Hereafter, the matrix $\mathcal{W}$ represents an orthonormal wavelet transform. Let $\widehat{\boldsymbol{d}} = \{\delta(c_i)\}_{1\leqslant i\leqslant N}$ be the sequence resulting from the shrinkage of $\{c_i\}_{1\leqslant i\leqslant N}$ by using a function $\delta(\cdot)$. We obtain an estimate of $\boldsymbol{f}$ by setting $\widehat{\boldsymbol{f}} = \mathcal{W}^{\mathsf{T}}\widehat{\boldsymbol{d}}$ where $\mathcal{W}^{\mathsf{T}}$ is the transpose, and thus, the inverse orthonormal wavelet transform.

In [13], the hard and soft-thresholding functions are proposed for wavelet coefficient estimation of a signal corrupted by Additive, White and Gaussian Noise (AWGN). Using these thresholding functions adjusted with suitable thresholds, [13] shows that, in AWGN, the wavelet-based estimators thus obtained achieve within a factor of $2\log N$ of the performance achieved with the aid of an oracle. Despite the asymptotic near-optimality of these standard thresholding functions, we have the following limitations. The hard-thresholding function is not everywhere continuous and its discontinuities generate a high variance of the estimate; on the other hand, the soft-thresholding function is continuous, but creates an attenuation on large coefficients, which results in an over-smoothing and an important bias for the estimate [9]. In practice, these thresholding functions (and their alternatives "non-negative garrote" function [14], "smoothly clipped absolute deviation" function [4]) yield musical noise in speech denoising and visual artifacts or over-smoothing of the estimate in image processing (see for instance the experimental results given in Section 4.1). Moreover, although thresholding rules are proved to be relevant strategies for estimating sparse signals [13], wavelet representations of many signals encountered in practical applications such as speech and image processing fail to be sparse enough (see illustrations given in [7, Figure 3]). For a signal whose wavelet representation fails to be sparse enough, it is more convenient to impose the penalized shrinkage condition **(P2)** instead of zero-forcing since small coefficients may contain significant information about the signal. Condition **(P1)** guarantees the regularity of the shrinkage process and the role of condition **(P3)** is to avoid over-smoothing of the estimate (noise mainly affect small wavelet coefficients). SigShrink functions are thus suitable functions for such an estimation since they satisfy **(P1)**, **(P2)** and **(P3)** conditions. The following addresses the optimization of the SigShrink parameters.

3.2 SURE-based optimization of SigShrink parameters

Consider the WaveShrink estimation described in section 3.1. The risk function or cost used to measure the accuracy of a WaveShrink estimator $\widehat{\boldsymbol{f}}$ of $\boldsymbol{f}$ is the standard MSE. Since the transform $\mathcal{W}$ is orthonormal, this cost is

$$r_\delta(\boldsymbol{d},\widehat{\boldsymbol{d}}) = \frac{1}{N}\mathbb{E}\|\boldsymbol{d}-\widehat{\boldsymbol{d}}\|^2 = \frac{1}{N}\sum_{i=1}^{N}\mathbb{E}\Big(d_i-\delta(c_i)\Big)^2 \tag{6}$$

for a shrinkage function δ. The SURE approach [22] involves estimating unbiasedly the risk $r_\delta(\boldsymbol{d},\widehat{\boldsymbol{d}})$. The SURE optimization then consists in finding the set of parameters that minimizes this unbiased estimate. The following result is a consequence of [16, Theorem 1].

Proposition 1 *The quantity $\vartheta + ||\boldsymbol{d}||^2_{\ell_2}/N$, where $||\cdot||_{\ell_2}$ denotes ℓ_2-norm and*

$$\vartheta(\tau,\lambda) = \frac{1}{N}\sum_{i=1}^{N}\frac{2\sigma^2 - c_i^2 + 2(\sigma^2+\sigma^2\tau|c_i|-c_i^2)e^{-\tau(|c_i|-\lambda)}}{(1+e^{-\tau(|c_i|-\lambda)})^2}, \tag{7}$$

is an unbiased estimator of the risk $r_{\delta_{\tau,\lambda}}(\boldsymbol{d},\widehat{\boldsymbol{d}})$, where $\delta_{\tau,\lambda}$ is a SigShrink function.

Proof: From [16, Theorem 1], we have that

$$r_\delta(\boldsymbol{d},\widehat{\boldsymbol{d}}) = \frac{1}{N}\left(||\boldsymbol{d}||^2_{\ell_2} + \sum_{i=1}^{N}\mathbb{E}\left(\delta^2(c_i) - 2c_i\delta(c_i) + 2\sigma^2\delta'(c_i)\right)\right), \tag{8}$$

where δ can be any differentiable shrinkage function that does not explode at infinity (see [16] for details). A SigShrink function is such a shrinkage function. Taking into account that the derivate of the SigShrink function $\delta_{\tau,\lambda}$ is

$$\delta'_{\tau,\lambda}(x) = \frac{1+(1+\tau|x|)e^{-\tau(|x|-\lambda)}}{(1+e^{-\tau(|x|-\lambda)})^2}, \tag{9}$$

the result derives from Eq. (1), Eq. (8) and Eq. (9). ∎

As a consequence of proposition 1, we get that minimizing $r_{\delta_{\tau,\lambda}}(\boldsymbol{d},\widehat{\boldsymbol{d}})$ of Eq. (6) amounts to minimizing the unbiased (SURE) estimator ϑ given by Eq. (7). The next section presents experimental tests for illustrating the SURE SigShrink denoising of some natural images corrupted by AWGN. For every tested image and every noise standard deviation considered, the optimal SURE SigShrink parameters are those minimizing ϑ, the vector $\boldsymbol{c}$ representing the wavelet coefficients of the noisy image.

3.3 Experimental results

The SURE optimization approach for SigShrink is now given for some standard test images corrupted by AWGN. We consider the standard 2-dimensional Discrete Wavelet Transform (DWT) by using the Symlet wavelet of order 8 ('sym8' in the Matlab Wavelet toolbox).

The SigShrink estimation is compared with that of the SURELET "sum of DOGs" (Derivatives Of Gaussian). SURELET (free MatLab software[1]) is a SURE-based method that moreover includes an inter-scale predictor with *a priori* information about the position of significant wavelet coefficients. For the comparison with SigShrink, we only use the "sum of DOGs" parameterization, that is the SURELET method without inter-scale predictor and Gaussian smoothing. By so proceeding, we thus compare two shrinkage functions: SigShrink and "sum of DOGs".

In the sequel, the SURE SigShrink parameters (attenuation degree and threshold) are those obtained by performing the SURE optimization on the whole set of the detail DWT coefficients. The attenuation degree and threshold thus computed are then applied at every decomposition level to the detail DWT coefficients. We also introduce the SURE Level-Dependent SigShrink (SURE LD-SigShrink) parameters. These parameters are obtained by applying a SURE optimization at every detail (horizontal, vertical, diagonal) sub-image located at the different resolution levels concerned (4 resolution levels in our experiments).

The tests are carried out with the following values for the noise standard deviation: $\sigma = 5, 15, 25, 35$. For every value σ, 25 tests have been performed based on different noise realizations. Every test involves: performing a DWT for the tested image corrupted by AWGN, computing the optimal SURE parameters (SigShrink and LD-SigShrink), applying the SigShrink function with these parameters to denoise the wavelet coefficients and building an estimate of the corresponding image by applying the inverse DWT to the shrunken coefficients. For every test, the PSNR is calculated for the original image and the denoised image. The

[1] avalaible at `http://bigwww.epfl.ch/demo/suredenoising/`

PSNR (in deciBel unit, dB), often used to assess the quality of a compressed image, is given by

$$\mathrm{PSNR} = 10\log_{10}\left(v^2/\mathrm{MSE}\right), \tag{10}$$

where v stands for the dynamics of the signal, $v = 255$ in the case of 8 bit-coded images.

Table 1 gives the following statistics for the 25 PSNRs obtained by the SURE SigShrink, SURE LD-SigShrink and "sum of DOGs" method: average value, variance, minimum and maximum. Average values and variances for the SURE SigShrink and SURE LD-SigShrink parameters are given in tables 2 - 3 - 4 - 5.

We use the Matlab routine `fmincon` to compute the optimal SURE SigShrink parameters. This function computes the minimum of a constrained multivariable function by using nonlinear programming methods (see Matlab help for the details). Note the following. First, one can use a test set and average the optimal parameter values on this set for application to images other than those used in the test set. By so proceeding, we avoid the systematic use of optimization algorithms such as `fmincon` on images that do not pertain to the test class. The low variability that holds among the optimal parameters given in tables 2 - 3 - 4 - 5 ensures the robustness of the average values. Second, instead of using optimal parameters, one can use heuristic ones (calculated by taking into account the physical meaning of these parameters and the noise statistical properties) such as the standard minimax or universal thresholds, which are shown to perform well with SigShrink (see Section 4 above).

From table 1, it follows that the 3 methods yield PSNRs of the same order. The level dependent strategy for SigShrink (LD-SigShrink) tends to achieve better results than the SigShrink and the "sum of DOGs". For every method, the difference (over the 25 noise realizations) between the minimum and maximum PSNR is less than 0.2 dB.

From tables 2 - 3 - 4 - 5, we observe (concerning the optimal SURE SigShrink parameters) that

- the threshold height, as well as the attenuation degree tend to be increasing functions of the noise standard deviation σ.
- for every tested σ, the SURE level-dependent attenuation degree and threshold tend to decrease when the resolution level increase (see table 4).
- for every fixed σ, the variance of the optimal SURE parameters over the 25 noise realizations is small: optimal parameters are not very disturbed for different noise realizations.
- as far as the level dependent strategy is concerned, the attenuation degree as well as the threshold tend to decrease when the resolution level increase for a fixed σ.

4 Smooth adaptation

In this section, we highlight specific features of SigShrink functions with respect to several issues in image processing.

Besides its simplicity (function with explicit close form, in contrast to parametric methods such as Bayesian shrinkages [21, 12, 11, 19, 15, 23]), the main features of the SigShrink functions in image processing are

Table 1: Means, variances, minima and maxima of the PSNRs computed over 25 noise realizations, when denoising test images by the SURE SigShrink, SURE LD-SigShrink and "sum of DOGs" methods. The tested images are corrupted by AWGN with standard deviation σ. The DWT is computed by using the 'sym8' wavelet. Some statistics are given in tables 2 - 3 - 4 - 5 for the SigShrink and LD-SigShrink optimal SURE parameters.

Image		'House'	'Peppers'	'Barbara'	'Lena'	'Flin'	'Finger'	'Boat'	'Barco'
$\sigma = 5$ ($\Longrightarrow$ Input PSNR = 34.1514).									
Mean(PSNR)	SigShrink	37.1570	36.4765	36.2587	37.3046	35.2207	35.3831	36.1187	36.6890
	LD-SigShrink	37.4880	36.6827	36.3980	37.5518	35.3128	35.8805	36.3608	36.9928
	SURELET	37.3752	36.6708	36.3767	37.5023	35.3102	35.9472	36.3489	35.9698
Var(PSNR) $\times 10^3$	SigShrink	0.4269	0.3635	0.0746	0.0696	0.0702	0.0630	0.0533	0.5338
	LD-SigShrink	0.8786	0.3081	0.0879	0.0643	0.0262	0.0571	0.0937	0.5613
	SURELET	0.5154	0.4434	0.0994	0.1241	0.0413	0.0453	0.0479	0.3132
Min(PSNR)	SigShrink	37.1067	36.4479	36.2409	37.2837	35.2021	35.3681	36.1060	36.6384
	LD-SigShrink	37.4427	36.6502	36.3764	37.5377	35.3043	35.8695	36.3409	36.9220
	SURELET	37.3196	36.6280	36.3502	37.4799	35.2986	35.9355	36.3353	35.9190
Max(PSNR)	SigShrink	37.2101	36.5211	36.2753	37.3202	35.2385	35.4043	36.1309	36.7345
	LD-SigShrink	37.5405	36.7100	36.4175	37.5750	35.3244	35.8985	36.3790	37.0374
	SURELET	37.4218	36.7061	36.3967	37.5198	35.3255	35.9614	36.3636	35.9960
$\sigma = 15$ ($\Longrightarrow$ Input PSNR = 24.6090).									
Mean(PSNR)	SigShrink	31.0833	29.5395	28.9750	31.3434	27.9386	28.1546	29.6099	29.9200
	LD-SigShrink	31.6472	30.0930	29.3972	32.0571	28.3815	29.4191	30.2895	30.4545
	SURELET	31.2834	29.9621	29.2817	31.9059	28.3502	29.4365	30.2706	27.4525
Var(PSNR)	SigShrink	0.0016	0.0010	0.0003	0.0003	0.0001	0.0002	0.0003	0.0019
	LD-SigShrink	0.0030	0.0009	0.0003	0.0008	0.0002	0.0002	0.0003	0.0015
	SURELET	0.0014	0.0008	0.0003	0.0004	0.0001	0.0002	0.0003	0.0005
Min(PSNR)	SigShrink	31.0022	29.4883	28.9490	31.3068	27.9221	28.1188	29.5829	29.8443
	LD-SigShrink	31.5005	30.0315	29.3741	31.9621	28.3647	29.3908	30.2563	30.3773
	SURELET	31.2056	29.9124	29.2378	31.8653	28.3339	29.3967	30.2468	27.4074
Max(PSNR)	SigShrink	31.1630	29.6216	29.0129	31.3777	27.9555	28.1724	29.6416	30.0088
	LD-SigShrink	31.7552	30.1848	29.4313	32.0952	28.4164	29.4604	30.3272	30.5144
	SURELET	31.3555	30.0225	29.3075	31.9350	28.3616	29.4571	30.3093	27.4843
$\sigma = 25$ ($\Longrightarrow$ Input PSNR = 20.1720).									
Mean(PSNR)	SigShrink	28.5549	26.5452	25.9539	28.7835	24.8761	25.1774	26.9844	27.2684
	LD-SigShrink	29.2948	27.3111	26.5146	29.7435	25.6407	26.6262	27.8216	27.9599
	SURELET	28.8085	26.9941	26.4404	29.5937	25.5953	26.7659	27.8227	23.6221
Var(PSNR)	SigShrink	0.0015	0.0009	0.0004	0.0007	0.0002	0.0002	0.0002	0.0017
	LD-SigShrink	0.0028	0.0022	0.0006	0.0013	0.0002	0.0003	0.0007	0.0024
	SURELET	0.0015	0.0024	0.0004	0.0004	0.0003	0.0003	0.0004	0.0006
Min(PSNR)	SigShrink	28.4563	26.4906	25.9164	28.7256	24.8499	25.1474	26.9606	27.1534
	LD-SigShrink	29.1894	27.2160	26.4642	29.6501	25.6143	26.5912	27.7927	27.8702
	SURELET	28.7439	26.8867	26.4128	29.5424	25.5599	26.7256	27.7803	23.5541
Max(PSNR)	SigShrink	28.6309	26.5974	25.9921	28.8215	24.8962	25.1962	27.0133	27.3490
	LD-SigShrink	29.4082	27.3887	26.5684	29.8135	25.6715	26.6726	27.8970	28.0518
	SURELET	28.8828	27.0884	26.4771	29.6331	25.6259	26.8062	27.8615	23.6703
$\sigma = 35$ ($\Longrightarrow$ Input PSNR = 17.2494).									
Mean(PSNR)	SigShrink	26.9799	24.6863	24.2771	27.1918	22.9274	23.3429	25.4271	25.7142
	LD-SigShrink	27.7840	25.5818	24.8910	28.2782	23.9326	24.9625	26.3764	26.5068
	SURELET	27.2768	25.1307	24.8383	28.1462	23.8954	25.0756	26.3880	21.3570
Var(PSNR)	SigShrink	0.0018	0.0014	0.0005	0.0011	0.0002	0.0002	0.0006	0.0020
	LD-SigShrink	0.0071	0.0035	0.0006	0.0022	0.0007	0.0003	0.0011	0.0035
	SURELET	0.0021	0.0012	0.0004	0.0008	0.0003	0.0003	0.0006	0.0007
Min(PSNR)	SigShrink	26.8957	24.6337	24.2299	27.1388	22.9031	23.3139	25.3856	25.6094
	LD-SigShrink	27.6242	25.4966	24.8499	28.1395	23.8746	24.9369	26.3102	26.3964
	SURELET	27.1928	25.0577	24.7906	28.0753	23.8608	25.0446	26.3167	21.3180
Max(PSNR)	SigShrink	27.0502	24.7740	24.3079	27.2623	22.9493	23.3813	25.4782	25.7942
	LD-SigShrink	27.9473	25.7515	24.9507	28.3628	23.9717	24.9984	26.4346	26.5985
	SURELET	27.3627	25.2000	24.8701	28.1867	23.9375	25.1146	26.4311	21.4116

Table 2: Mean values (based on 25 noise realizations) for optimal DWT 'sym8' SURE SigShrink parameters, when denoising the 'Lena' image corrupted by AWGN. The SURE SigShrink parameters are the SigShrink parameters θ and λ obtained by performing the SURE optimization on the whole set of the detail DWT coefficients. It follows from these results that the threshold height, as well as the attenuation degree tend to be increasing functions of the noise standard deviation σ.

Image:	'House'	'Peppers'	'Barbara'	'Lena'	'Flinstones'	'Fingerprint'	Boat	'Barco'
$\sigma = 5$								
Mean θ :	0.3183	0.2615	0.2655	0.3054	0.1309	0.1309	0.1913	0.3122
Mean λ/σ :	2.3420	1.9289	1.9156	2.3861	1.1145	1.1375	1.6885	2.1334
$\sigma = 15$								
Mean θ :	0.5113	0.4407	0.4256	0.5158	0.3429	0.3491	0.4264	0.4584
Mean λ/σ :	3.0439	2.6016	2.6259	3.1045	2.3897	2.4181	2.8454	2.8954
$\sigma = 25$								
Mean θ :	0.5640	0.4931	0.4638	0.5764	0.4305	0.4310	0.4997	0.5185
Mean λ/σ :	3.2612	2.7893	2.9397	3.3283	2.7167	2.7670	3.1414	3.2043
$\sigma = 35$								
Mean θ :	0.5925	0.5151	0.4900	0.6066	0.4761	0.4802	0.5389	0.5505
Mean λ/σ :	3.3885	2.9240	3.2249	3.4733	2.8835	2.9493	3.3459	3.4142

Table 3: Variances (based on 25 noise realizations) for the optimal SURE SigShrink parameters whose means are given in table 2.

Image:	'House'	'Peppers'	'Barbara'	'Lena'	'Flinstones'	'Fingerprint'	Boat	'Barco'
$\sigma = 5$								
Var $\theta : 10^{-04} \times$	0.1550	0.2625	0.0877	0.0592	0.0002	0.0004	0.0642	0.2138
Var $\lambda/\sigma : 10^{-03} \times$	0.0932	0.2204	0.0591	0.0209	0.0015	0.0017	0.1454	0.1500
$\sigma = 15$								
Var $\theta : 10^{-04} \times$	0.4569	0.2777	0.0468	0.1946	0.0722	0.0297	0.0478	0.5645
Var λ/σ :	0.0002	0.0001	0.0003	0.0011	0.0003	0.0003	0.0018	0.0001
$\sigma = 25$								
Var $\theta : 10^{-04} \times$	0.4858	0.3753	0.0968	0.1594	0.0433	0.0586	0.1100	0.6510
Var $\lambda/\sigma : 10^{-03} \times$	0.6270	0.1439	0.0504	0.1215	0.0184	0.0227	0.0452	0.3095
$\sigma = 35$								
Var $\theta : 10^{-04} \times$	0.7011	0.3639	0.1123	0.2463	0.0662	0.1041	0.0982	0.8360
Var $\lambda/\sigma : 10^{-03} \times$	0.9610	0.4325	0.1219	0.1720	0.2287	0.0445	0.1570	0.7928

Table 4: Mean values of the optimal SURE LD-SigShrink parameters, for the denoising of the 'Lena' image corrupted by AWGN. The DWT with the 'sym8' wavelet is used. The SURE LD-SigShrink parameters are obtained by applying a SURE optimization at every detail (Hori. for Horizontal, Vert. for Vertical, Diag. for Diagonal) sub-image located at the different resolution levels concerned. We remark first that the threshold height, as well as the attenuation degree, tend to be increasing functions of the noise standard deviation σ. In addition, for every σ considered, the attenuation degree as well as the threshold tend to decrease when the resolution level increase.

$\sigma = 5$						
	θ			λ/σ		
	Hori.	Vert.	Diag.	Hori.	Vert.	Diag.
$J = 1$	0.2864	0.2738	0.3172	3.1072	2.3829	4.2136
$J = 2$	0.2298	0.1722	0.3057	1.8747	1.4181	2.1687
$J = 3$	0.0863	0.0657	0.1868	0.7361	0.4852	1.3251
$J = 4$	0.1154	0.1558	0.4071	0.4957	0.4867	1.4383

$\sigma = 15$						
	θ			λ/σ		
	Hori.	Vert.	Diag.	Hori.	Vert.	Diag.
$J = 1$	0.5397	0.4517	0.9361	4.9893	4.0930	4.6560
$J = 2$	0.4209	0.3767	0.4641	2.9436	2.4534	3.1053
$J = 3$	0.2622	0.1794	0.3481	1.9541	1.3087	2.2195
$J = 4$	0.2128	0.3161	0.4528	1.0539	1.0125	1.8657

$\sigma = 25$						
	θ			λ/σ		
	Hori.	Vert.	Diag.	Hori.	Vert.	Diag.
$J = 1$	0.8934	0.5412	0.9712	4.5129	5.0167	4.4367
$J = 2$	0.4633	0.4217	0.5209	3.5723	2.8134	3.8653
$J = 3$	0.3294	0.2642	0.4135	2.4032	1.7920	2.5764
$J = 4$	0.2644	0.3264	0.4655	1.5004	1.3231	2.0720

$\sigma = 35$						
	θ			λ/σ		
	Hori.	Vert.	Diag.	Hori.	Vert.	Diag.
$J = 1$	0.8772	0.8785	0.9575	4.6843	4.5268	4.6499
$J = 2$	0.4963	0.4389	0.5746	4.2031	3.2062	4.5700
$J = 3$	0.3643	0.2745	0.4424	2.6642	1.9881	2.8343
$J = 4$	0.2700	0.3119	0.4743	1.6543	1.3744	2.2185

Table 5: Variances (based on 25 noise realizations) for optimal SURE SigShrink parameters whose means are given in table 4.

$\sigma = 5$						
	θ			λ/σ		
	Hori.	Vert.	Diag.	Hori.	Vert.	Diag.
$J = 1$	4.0132×10^{-05}	2.3941×10^{-05}	7.8842×10^{-05}	3.2225×10^{-04}	1.2107×10^{-04}	1.2801×10^{-02}
$J = 2$	7.1936×10^{-05}	9.1042×10^{-05}	8.2755×10^{-05}	8.9961×10^{-04}	2.1122×10^{-02}	3.3873×10^{-04}
$J = 3$	3.9358×10^{-04}	1.9894×10^{-06}	4.9047×10^{-04}	1.7802×10^{-02}	9.4616×10^{-05}	8.1475×10^{-03}
$J = 4$	3.8724×10^{-02}	7.2803×10^{-02}	1.0830×10^{-02}	2.6745×10^{-02}	4.4741×10^{-02}	9.0581×10^{-03}

$\sigma = 15$						
	θ			λ/σ		
	Hori.	Vert.	Diag.	Hori.	Vert.	Diag.
$J = 1$	1.1386×10^{-05}	8.5503×10^{-05}	2.9411×10^{-02}	9.1445×10^{-04}	5.2059×10^{-03}	1.7085×10^{-01}
$J = 2$	1.2669×10^{-04}	1.0311×10^{-04}	1.8030×10^{-04}	3.1178×10^{-04}	3.7783×10^{-04}	1.3153×10^{-03}
$J = 3$	7.0001×10^{-04}	9.6295×10^{-04}	4.0143×10^{-03}	5.8012×10^{-03}	1.7847×10^{-02}	1.1231×10^{-03}
$J = 4$	3.5209×10^{-02}	8.4438×10^{-02}	4.7492×10^{-03}	6.0936×10^{-02}	1.2701×10^{-01}	5.4097×10^{-03}

$\sigma = 25$						
	θ			λ/σ		
	Hori.	Vert.	Diag.	Hori.	Vert.	Diag.
$J = 1$	3.6502×10^{-03}	6.7723×10^{-05}	1.3148×10^{-02}	3.2220×10^{-01}	3.0924×10^{-03}	3.718×10^{-01}
$J = 2$	2.2414×10^{-04}	1.5173×10^{-04}	4.5237×10^{-04}	3.7254×10^{-03}	4.2258×10^{-04}	1.5425×10^{-02}
$J = 3$	5.9582×10^{-04}	2.5486×10^{-05}	4.3791×10^{-04}	2.6453×10^{-02}	8.5859×10^{-04}	8.3580×10^{-04}
$J = 4$	1.0268×10^{-04}	1.8425×10^{-02}	3.0014×10^{-02}	2.9073×10^{-02}	7.6271×10^{-03}	3.6192×10^{-03}

$\sigma = 35$						
	θ			λ/σ		
	Hori.	Vert.	Diag.	Hori.	Vert.	Diag.
$J = 1$	2.2438×10^{-02}	3.7058×10^{-02}	1.1533×10^{-02}	2.7270×10^{-01}	2.6113×10^{-01}	2.8441×10^{-01}
$J = 2$	4.7551×10^{-04}	2.7514×10^{-04}	9.0224×10^{-04}	4.2308×10^{-02}	2.0487×10^{-03}	9.8234×10^{-02}
$J = 3$	9.0951×10^{-04}	2.1239×10^{-04}	8.5623×10^{-04}	3.2461×10^{-03}	1.2198×10^{-03}	3.4412×10^{-03}
$J = 4$	5.9373×10^{-04}	9.1487×10^{-03}	2.8074×10^{-03}	4.2265×10^{-03}	5.6180×10^{-03}	4.9168×10^{-03}

Adjustable denoising: the flexibility of the SigShrink parameters allows to choose the denoising level. From hard denoising (degenerated SigShrink) to smooth denoising, there exists a wide class of regularities that can be attained for the denoised signal by adjusting the attenuation degree and threshold.

Artifact-free denoising: the smoothness of the non-degenerated SigShrink functions allows for reducing noise without impacting significantly the signal: a better preservation of the signal characteristics (visual perception) and its statistical properties is guaranteed due to the fact that the shrinkage is performed with less variability among coefficients with close values.

Contrast function: the SigShrink function and its inverse, the SigStretch function, can be seen as contrast functions. The SigShrink function enhances contrast, whereas the SigStretch function reduces contrast).

Below, we detail these characteristics. The following proposition characterizes the SigStretch function.

Proposition 2 *The SigStretch function, denoted $r_{\tau,\lambda}$, is defined as the inverse of the SigShrink function $\delta_{\tau,\lambda}$ and is given by*

$$r_{\tau,\lambda}(z) = z + \operatorname{sgn}(z)\mathscr{L}\left(\tau|z|e^{-\tau(|z|-\lambda)}\right)/\tau \tag{11}$$

for any real value z, with $\mathscr{L}$ being the Lambert function defined as the inverse of the function: $t \geqslant 0 \longmapsto te^t$.

Proof: [See appendix]. ∎

In the rest of the paper, the wavelet transform used is the Stationary (also call shift-invariant or redundant) Wavelet Transform (SWT) [10]. This transform has appreciable properties in denoising. Its redundancy makes it possible to reduce residual noise due to the translation sensitivity of the orthonormal wavelet transform.

4.1 Adjustable and artifact-free denoising

The shrinkage performed by the SigShrink method is adjustable *via* the attenuation degree θ and the threshold λ.

Figures 4 and 5 give denoising examples for different values of θ and λ. The denoising concerns the 'Lena' image corrupted by AWGN with standard deviation $\sigma = 35$ (figure 3). The 'Haar' wavelet and 4 decomposition levels are used for the wavelet representation (SWT). The classical minimax and universal thresholds [13] are used. In these figures, SigShrink$_{\theta,\lambda}$ stands for the SigShrink function which parameters are θ and λ.

For a fixed attenuation degree, we observe that the smoother denoising is obtained with the larger threshold (universal threshold). Small value for the threshold (minimax threshold) leads to better preservation of the textural information contained in the image (compare in figure 4, image (a) versus image (d); image (b) versus image (e); image (c) versus image (f); or equivalently, compare the zooms of these images shown in figure 5).

Now, for a fixed threshold λ, the SigShrink shape is controllable *via* θ (see figure 2). The attenuation degree θ, $0 < \theta < \arccos(\sqrt{5}/5)$, reflects the regularity of the shrinkage and the attenuation imposed to data

with small amplitudes (mainly noise coefficients). The larger θ, the more the noise reduction. However, SigShrink functions are more regular for small values of θ, and thus, small values for θ lead to less artifacts (in figure 5, compare images (d), (e) and (f).

It follows that SigShrink denoising is flexible thanks to parameters λ and θ, preserves the image features and leads to artifact-free denoising. It is thus possible to reduce noise without impacting the signal characteristics significantly. Artifact free denoising is relevant in many applications, in particular for medical imagery where visual artifacts must be avoided. In this respect, we henceforth consider small values for the attenuation degree.

Note that the SURELET "sum of DOGs" parameterization does not allow for such an heuristically adjustable denoising because the physical interpretation of its parameters is not explicit, whereas the SigShrink and the standard hard, soft, NNG and SCAD thresholding functions mentioned in Section 3.1 depend on parameters with more intuitive physical meaning (threshold height and an additional attenuation degree parameter for SigSghink). Denoising examples achieved by using the hard, soft, NNG and SCAD thresholding functions are given in figure 6, for a comparison with the SigShrink denoising. The minimax threshold is used for the denoising (the results are even worse with the universal threshold). As can be seen in this figure, artifacts are visible in the image denoised by using hard-thresholding, whereas images denoised by using soft, NNG and SCAD thresholding functions tend to be over-smoothed. Numerical comparison of the denoising PSNRs performed by SigShrink and these standard thresholding functions can be found in [8].

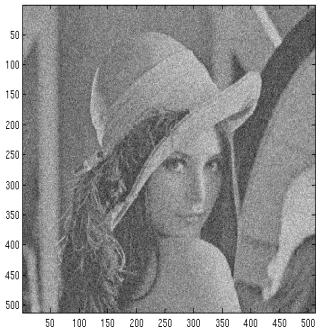

Figure 3: Noisy 'Lena' image, noise is AWGN with standard deviation $\sigma = 35$, which corresponds to an input PSNR=17.2494 dB.

Remark 1 *At this stage, it is worth mentioning the following. Some parametric shrinkages using a priori distributions for modeling the signal wavelet coefficients can sometimes be described by non-parametric functions with explicit formulas (for instance, a Laplacian assumption leads to a soft-thresholding shrinkage). In this respect, one can wonder about possible links between SigShrink and the Bayesian Sigmoid Shrinkage (BSS) of [23]. BSS is a one-parameter family of shrinkage functions, whereas SigShrink functions depend on two parameters. Fixing one of these two parameters yields a sub-class of SigShrink functions. It is then reasonable to think that, depending on the distribution of the signal and noise wavelet coefficients, these functions should somehow relate to BSS. Actually, such a possible link has not yet been established.*

Figure 4: SWT SigShrink denoising of 'Lena' image corrupted by AWGN with standard deviation $\sigma = 35$. The universal threshold λ_u and the minimax threshold λ_m are used. The universal threshold (the larger threshold) yields a smoother denoising, whereas the minimax threshold leads to better preservation of the textural information contained in the image.

(a) SigShrink$_{\pi/6,\lambda_u}$
PSNR=27.3019 dB

(b) SigShrink$_{\pi/4,\lambda_u}$
PSNR=27.0110 dB

(c) SigShrink$_{\pi/3,\lambda_u}$
PSNR=26.8441 dB

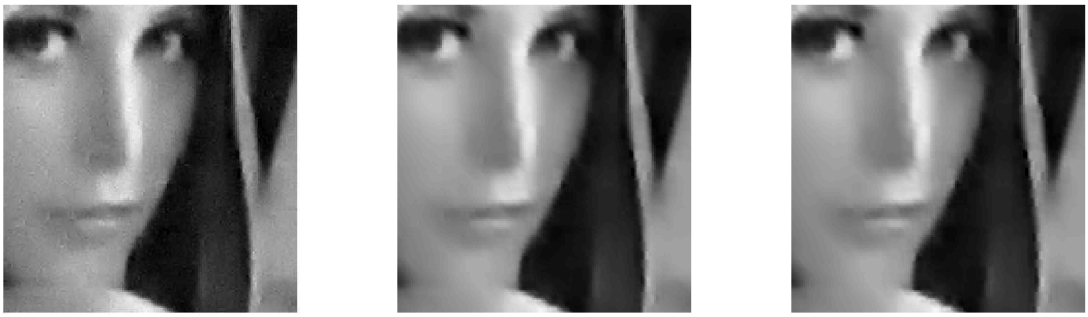

(d) SigShrink$_{\pi/6,\lambda_m}$
PSNR=27.2852 dB

(e) SigShrink$_{\pi/4,\lambda_m}$
PSNR=28.1485 dB

(f) SigShrink$_{\pi/3,\lambda_m}$
PSNR=27.9440 dB

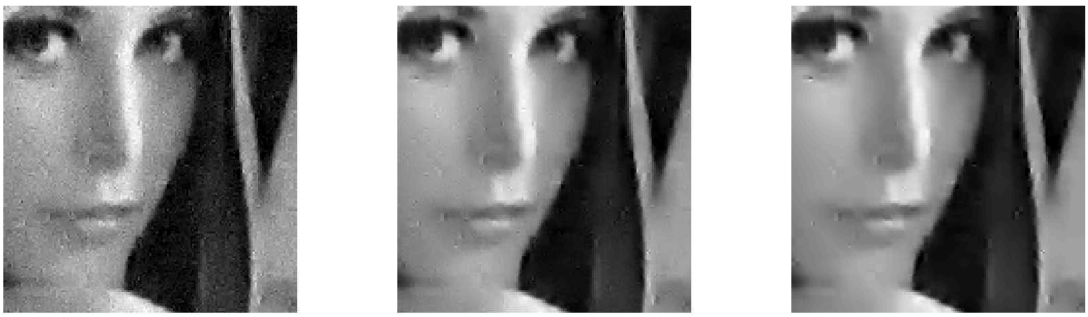

Figure 5: Zoom of the SigShrink denoising of 'Lena' images of figure 4.

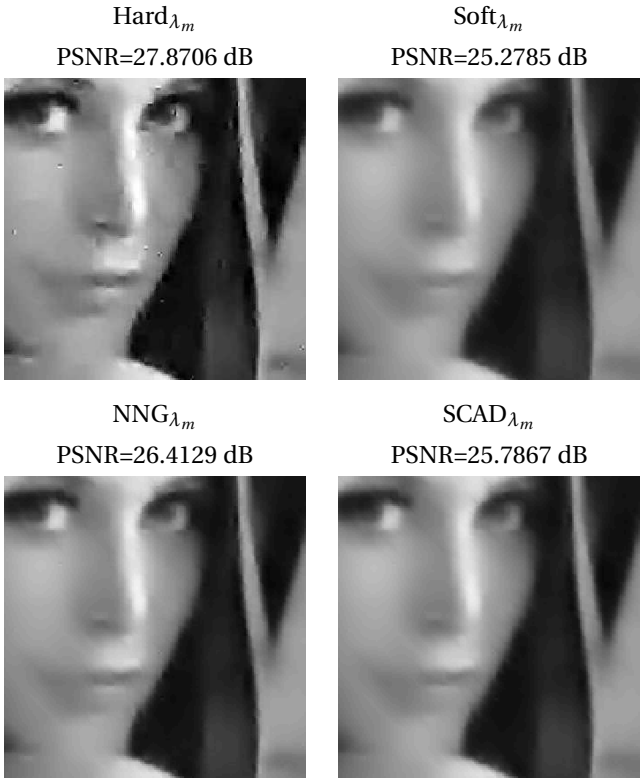

Figure 6: Denoising examples by using standard thresholding functions. The 'Haar' wavelet and 4 decomposition levels are used for the wavelet representation (SWT). The denoising concerns the image of figure 3.

To conclude this section, note that shrinkages and regularization procedures are linked in the sense that a shrinkage function solves to a regularization problem constrained by a specific penalty function [3]. Since SigShrink functions satisfy assumptions of [3, Proposition 3.2], the shrinkage obtained by using a function $\delta_{\tau,\lambda}$ can be seen as a regularization approximation [4] by seeking the vector $\boldsymbol{d}$ that minimizes the penalized least squares

$$||\boldsymbol{d}-\boldsymbol{c}||_{\ell_2}^2 + 2\sum_{i=1}^{N} q_{\tau,\lambda}(|d_i|), \tag{12}$$

where $q_\lambda = q_{\tau,\lambda}(\cdot)$ is the penalty function associated with $\delta_{\tau,\lambda}$, $q_{\tau,\lambda}$ is defined for every $x \geqslant 0$ by

$$q_{\tau,\lambda}(x) = \int_0^x (r_{\tau,\lambda}(z) - z)\mathrm{d}z, \tag{13}$$

with $r_{\tau,\lambda}$ the SigStretch function (inverse of the SigShrink function $\delta_{\tau,\lambda}$, see Eq. (11)). Thus, SigShrink have several interpretations depending on the model used.

4.2 Speckle denoising

In SAR, oceanography and medical ultrasonic imagery, sensors record many gigabits of data per day. These images are mainly corrupted by speckle noise. If post-processing such as segmentation or change detection

have to be performed on these databases, it is essential to be able to reduce speckle noise without impacting the signal characteristics significantly. The following illustrates that SigShrink makes it possible to achieve this because of its flexibility (see the shapes of SigShrink functions given in figure 2) and the artifact-free denoising they perform (see figures 4 - 5). In addition, since SigShrink is invertible, it is not essential to store a copy of the original database (thousands and thousands of gigabits recorded every year): one can retrieve an original image by simply applying the inverse SigShrink denoising procedure (SigStrech functions). More precisely, the following illustrates that SigShrink performs well for denoising speckle noise in the wavelet domain.

Speckle noise is a multiplicative type noise inherent to signal acquisition systems using coherent radiation. This multiplicative noise is usually modeled as a correlated stationary random process independent of the signal reflectance.

Two different additive representations are often used for speckle noise. The first model is a "signal-dependent" stationary noise model: noise, assumed to be stationary, depends on the signal reflectance. This model is simply obtained by noting that $\epsilon z = z + z(\epsilon - 1)$, z being the signal reflectance and ϵ being a stationary random process independent of z. The second model is a "signal-independent" model obtained by applying a logarithmic transform to the noisy image.

We begin with the speckle signal-dependent model. The denoising procedure then involves applying an SWT to the noisy image, estimating the noise standard deviation in each SWT subband by the robust MAD (Median of the Absolute Deviation, normalized by the constant 0.6745) estimator [13], shrinking the wavelet coefficients by using a SigShrink function adjusted with the minimax threshold [13], and reconstructing an estimate of the signal by means of the inverse SWT. The results obtained for the 'Lena' image corrupted by speckle noise (figure 7 (a)) are shown in figure 7 (b) - (c).

In addition, we consider the speckle signal-independent model. We use the estimation procedure described above for denoising the logarithmic transformed noisy image. The results are given in figure 7 (d) - (e).

By comparing the results of figure 7, we observe that the PSNRs achieved are of the same order whatever the model. However, the denoising obtained with the additive independent noise model (logarithmic transform) has a better visual quality than that obtained with the additive signal-dependent speckle model. In fact, one can note, from this figure, the ability of SigShrink functions to reduce speckle noise without impacting structural features and textural information of the image. Note also the gain in PSNR larger than 10 dBs, performance of the same order as that of the best up-to-date speckle denoising techniques ([24, 5, 2, 6, 1, 20] among others).

4.3 Contrast function

To conclude this section, we now present the SigShrink and SigStretch functions as contrast functions. Contrast functions are very useful in medical image processing. As a matter of fact, medical monitoring for arthroplasty (replacement of certain bone surfaces by implants due to lesions of the articular surfaces) requires 2D-3D registration of the implant, and thus, requires knowing exactly the position of the implant contour. Precise edge detection is no easy task [18] because edge detection methods are sensitive to contrast (global contrast for the image and local contrast around a contour). The following briefly describes

(a) Noisy image

PSNR = 18.8301 dB

Denoising without logarithmic transform

(b) SigShrink$_{\pi/6,\lambda_m}$

PSNR = 29.0078 dB

(c) SigShrink$_{\pi/4,\lambda_m}$

PSNR = 29.4059 dB

Denoising with logarithmic transform

(d) SigShrink$_{\pi/6,\lambda_m}$

PSNR = 29.0567 dB

(e) SigShrink$_{\pi/4,\lambda_m}$

PSNR = 29.2328 dB

Figure 7: SigShrink denoising of the 'Lena' image corrupted by speckle noise. The SWT with four resolution levels and the Haar filters are used. The noise standard deviation is estimated by the MAD normalized by the constant 0.6745 (see [13]).

how to use SigShrink - SigStretch functions as contrast functions.

The SigShrink function applies a penalized shrinkage to data with small amplitudes. The smaller the data amplitude, the higher the attenuation imposed by the SigShrink function. Thus, a SigShrink function is a contrast enhancing function: this function increases the gap between large and small values for the pixels of an image. As a consequence, a SigStretch function reduces the contrast by lowering the variation between large and small pixel values in the image. Figure 8 gives the original 'Lena' image, as well as the SigShrink $\delta_{\pi/6,100}$ and SigStretch $r_{\pi/6,100}$ shrunken images. This figure highlights that the contrast of the image can be smoothly adjusted (enhancement, reduction) by applying SigShrink and SigStretch functions without introducing artifacts. Note that, as for denoising, SigShrink allows for choosing the attenuation degree imposed to the data, when the threshold height is fixed. Figure 9 illustrates the variability that can be attained by varying the SigShrink attenuation degree for enhancing the contrast of a fluoroscopic image.

To conclude this section, we now illustrate the combination of SigShrink denoising and contrast enhancement for an ultrasonic image of breast cancer. The combination involves denoising the image by using the SigShrink method in the wavelet domain. A SigShrink function is then applied to the denoised image to enhance its contrast. The results are presented in figure 10. It is shown that SigShrink denoises the image and preserves feature information without introducing artifacts. The parameter $\theta = \pi/6$ is chosen so as to avoid visual artifacts. Different thresholds are experimented to highlight how we can progressively reduce noise without affecting the image textural information. The threshold λ_d is the detection threshold of [7]. This threshold is smaller than the minimax threshold. It is close to $\lambda_u/2$ when the sample size is large.

(a) SigStretch$_{\pi/6,100}$ (b) Original image (c) SigShrink$_{\pi/6,100}$

Figure 8: SigStretch and SigShrink applied on the 'Lena' image.

5 Conclusion

This work proposes the use of SigShrink - SigStretch functions for practical engineering problems such as image denoising, image restoration and image enhancement. These functions perform adjustable adaptation of data in the sense that they can enhance or reduce the variability among data, the adaptation process being regular and invertible. Because of the smoothness of the function used (infinitely differentiable in $]0,+\infty[$), the data adaptation is performed with little variability so that the signal characteristics are better

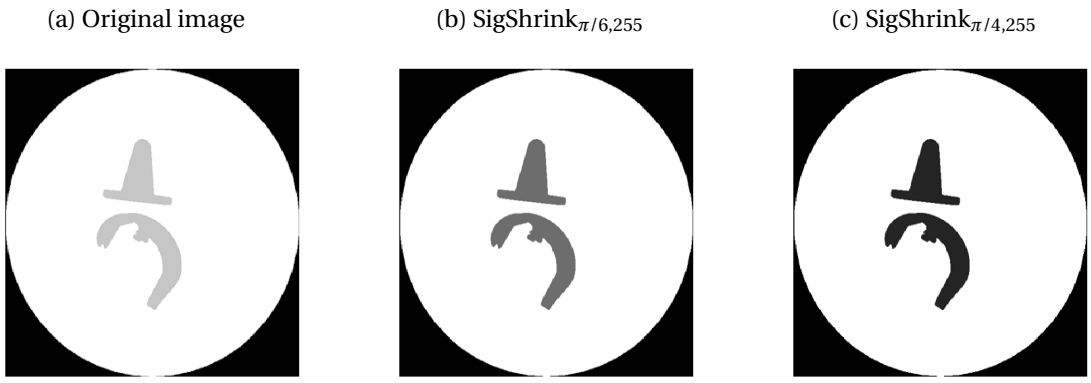

Figure 9: SigStretch and SigShrink applied on a fluoroscopic image.

preserved. The SigShrink and SigStretch methods are simple and flexible in the sense that the parameters of these classes of functions allow for a fine tuning of the data adaptation. This adaptation is non-parametric because no prior information about the signal is taken into account. A SURE based optimization of the parameters is possible.

The denoising achieved by a SigShrink function is almost artifact-free due to the little variability introduced among data with close amplitudes. This artifact-free denoising is relevant for many applications, in particular for medical imagery where visual artifacts must be avoided. In addition, a fine calibration of SigShrink parameters allows noise reduction without impacting the signal characteristics. This is important when some post-processing (such as a segmentation) must be performed on the signal estimate.

As far as perspectives are concerned, we can reasonably expect to improve SigShrink denoising performance by introducing inter-scale or/and intra-scale predictor, which could provide information about the position of significant wavelet coefficients. It could also be relevant to undertake a complete theoretical and experimental comparison between SigShrink and Bayesian sigmoid shrinkage [23].

In addition, application of SigShrink to speech processing could also be considered. Since SigShrink yields denoised images that are almost artifact-free, would it be possible that such an approach denoises speech signals corrupted by AWGN without returning musical noise, in contrast to classical shrinkages using thresholding rules?

Another perspective is the SigShrink - SigStretch calibration of contrast in order to improve edge detection in medical imagery. Exact edge detection is necessary for 2D-3D registration of images. Sub-pixel measurement of edge is possible by using for example the moment-based method of [17]. However, the method is very sensible to contrast. Low contrast varying images result in multiple contours, whereas high varying contrast in image leads to good precision for certain contour points, but induces lack of detection for points in lower contrast zones. The idea is the use of the SigShrink - SigStretch functions for improving image contrast so as to alleviate edge detection in medical imagery. For instance, we can expect that combining SigShrink - SigStretch with edge detection methods such as [17] can lead to good sub-pixel measurement of the contour in an image.

(a) Ultrasonic image

SigShrink denoising without contrast enhancement

(b) SigShrink$_{\pi/6,\lambda_d}$ (c) SigShrink$_{\pi/6,\lambda_m}$ (d) SigShrink$_{\pi/6,\lambda_u}$



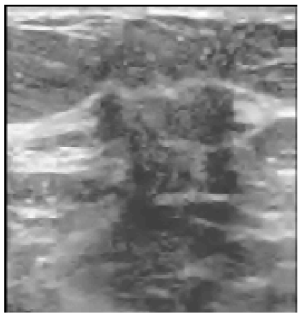

SigShrink denoising combined with SigShrink$_{\pi/6,100}$ contrast enhancement

(e) SigShrink$_{\pi/6,\lambda_d}$ (f) SigShrink$_{\pi/6,\lambda_m}$ (g) SigShrink$_{\pi/6,\lambda_u}$



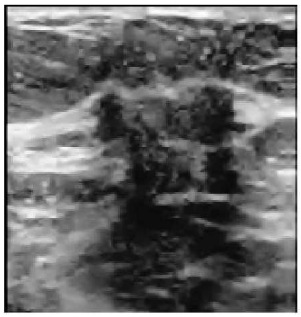

Figure 10: SigShrink denoising for an ultrasonic image of breast cancer. The SWT with four resolution levels and the biorthogonal spline wavelet with order 3 for decomposition and with order 1 for reconstruction ('bior1.3' in Matlab Wavelet toolbox) are used. The noise standard deviation is estimated by the MAD normalized by the constant 0.6745 (see [13]).

References

[1] A. Achim, E. E. Kuruoglu, and J. Zerubia. Sar image filtering based on the heavy-tailed rayleigh model. *IEEE Transactions on Image Processing*, 15(9):2686 – 2693, Sept. 2006.

[2] A. Achim, P. Tsakalides, and A. Bezerianos. Sar image denoising via bayesian wavelet shrinkage based on heavy-tailed modeling. *IEEE Transactions on Geoscience and Remote Sensing*, 41(8):1773 – 1784, Aug. 2003.

[3] A. Antoniadis. Wavelet methods in statistics: Some recent developments and their applications. *Statistics Surveys*, 1:16–55, 2007.

[4] A. Antoniadis and J. Fan. Regularization of wavelet approximations. *Journal of the American Statistical Association*, 96(455):939–955, Sep. 2001.

[5] F. Argenti and L. Alparone. Speckle removal from sar images in the undecimated wavelet domain. *IEEE Transactions on Geoscience and Remote Sensing*, 40(11):2363 – 2374, Nov. 2002.

[6] F. Argenti, T. Bianchi, and L. Alparone. Multiresolution map despeckling of sar images based on locally adaptive generalized gaussian pdf modeling. *IEEE Transactions on Image Processing*, 15(11):3385 – 3399, Nov. 2006.

[7] A. M. Atto, D. Pastor, and G. Mercier. Detection threshold for non-parametric estimation. *Signal, Image and Video Processing, Springer*, 2(3), Sept. 2008.

[8] A. M. Atto, D. Pastor, and G. Mercier. Smooth sigmoid wavelet shrinkage for non-parametric estimation. *IEEE International Conference on Acoustics, Speech, and Signal Processing, ICASSP*, Las Vegas, Nevada, USA, 30 march - 4 april, 2008.

[9] A. G. Bruce and H. Y. Gao. Understanding waveshrink: Variance and bias estimation. *Biometrika*, 83(4):727–745, 1996.

[10] R. R. Coifman and D. L. Donoho. *Translation invariant de-noising*, pages 125–150. Number 103. Lecture Notes in Statistics, 1995.

[11] L. Şendur and I. V. Selesnick. Bivariate shrinkage functions for wavelet-based denoising exploiting interscale dependency. *IEEE Transactions on Signal Processing*, 11:2744–2756, Nov. 2002.

[12] M. N. Do and M. Vetterli. Wavelet-based texture retrieval using generalized gaussian density and kullback-leibler distance. *IEEE Transactions on Image Processing*, 11(2):146–158, Feb. 2002.

[13] D. L. Donoho and I. M. Johnstone. Ideal spatial adaptation by wavelet shrinkage. *Biometrika*, 81(3):425–455, Aug. 1994.

[14] H. Y. Gao. Waveshrink shrinkage denoising using the non-negative garrote. *Journal of Computational and Graphical Statistics*, 7(4), 1998.

[15] I. M. Johnstone and B. W. Silverman. Empirical bayes selection of wavelet thresholds. *Annals of Statistics*, 33(4):1700–1752, 2005.

[16] F. Luisier, T. Blu, and M. Unser. A new sure approach to image denoising: Interscale orthonormal wavelet thresholding. *IEEE Transactions on Image Processing*, 16(3):593–606, Mar. 2007.

[17] E. P. Lyvers, O. R. Mitchell, M. L. Akey, and A. P. Reeves. Subpixel measurements using a moment-based edge operator. *IEEE Transactions on Pattern Analysis and Machine Intelligence*, 11(12):1293 – 1309, Dec. 1989.

[18] M. Mahfouz, W. Hoff, R. Komistek, and D. Dennis. Effect of segmentation errors on 3d-to-2d registration of implant models in x-ray images. *Journal of Biomechanics*, 38(2):229 – 239, 2004.

[19] J. Portilla, V. Strela, M. J. Wainwright, and E. P. Simoncelli. Image denoising using scale mixtures of gaussians in the wavelet domain. *IEEE Transactions on Image processing*, 12(11):1338–1351, November 2003.

[20] D. Sen, M. N. S. Swamy, and M. O. Ahmad. Computationally fast techniques to reduce awgn and speckle in videos. *IET Image Processing*, 1(4):319 – 334, 2007.

[21] E. P. Simoncelli and E. H. Adelson. Noise removal via bayesian wavelet coring. *IEEE Int. Conf. Image Proc. (ICIP)*, pages 379–382, Oct. 1996.

[22] C. Stein. Estimation of the mean of a multivariate normal distribution. *The Annals of Statistics*, 9:1135–1151, 1981.

[23] C. J. F. ter Braak. Bayesian sigmoid shrinkage with improper variance priors and an application to wavelet denoising. *Computational Statistics and Data Analysis*, 51(2):1232–1242, 2006.

[24] H. Xie, L. E. Pierce, and F. T. Ulaby. Sar speckle reduction using wavelet denoising and markov random field modeling. *IEEE Transactions on Geoscience and Remote Sensing*, 40(10):2196 – 2212, Oct. 2002.

Proof of Proposition 2

Because $\delta_{\tau,\lambda}$ is antisymmetric, $r_{\tau,\lambda}$ has the form

$$r_{\tau,\lambda}(z) = zG(z), \tag{14}$$

for every real value z and where G is such that

$$G(z) = 1 + e^{-\tau(|z|G(z)-\lambda)}.$$

Therefore, $G(z) > 1$ for any real value z. We thus have

$$(G(z)-1)\, e^{\tau(|z|(G(z)-1)} = e^{-\tau(|z|-\lambda)},$$

which is also equivalent to

$$\tau|z|\,(G(z)-1)\, e^{\tau(|z|(G(z)-1)} = \tau|z|e^{-\tau(|z|-\lambda)}.$$

It follows that

$$\tau|z|\,(G(z)-1) = \mathscr{L}\left(\tau|z|e^{-\tau(|z|-\lambda)}\right),$$

which leads to

$$G(z) = 1 + \mathscr{L}\left(\tau|z|e^{-\tau(|z|-\lambda)}\right)/(\tau|z|) \tag{15}$$

for $z \neq 0$. The result then follows from (14), (15) and the fact that $r_{\tau,\lambda}(0) = 0$ since $\delta_{\tau,\lambda}(0) = 0$.